

The Algorithms of Urban Sprawl Dynamics on Surface Temperature Characteristics of Greater Port Harcourt Region, Using Remote Sensing- GIS Approach

Vincent Ezikornwor Weli^{1*}, Alexander Chibuzor Okoli¹ and Shedrach Worlu²

¹Department of Geography and Environmental Management, University of Port-Harcourt, Choba, Port Harcourt, Nigeria

²Department of Social Studies, Federal College of Technical, Omoku, Nigeria

***Corresponding Author:** Vincent Ezikornwor Weli, Department of Geography and Environmental Management, University of Port-Harcourt, Choba, Port Harcourt, Nigeria

ABSTRACT

Urbanization has global notable alteration on thermal, radiative, moisture and aerodynamic features of the landscape, which adversely affects the surface energy balance within the atmosphere. These alterations can propel a higher air and surface temperature of the urban centres when compared with the surrounding environment which is typically termed as urban heat island. In this study GIS and remote sensing were used to evaluate urban sprawl variation on surface temperature in Greater Port Harcourt. Landsat Thematic Mapper (TM), Enhanced Thematic Mapper plus (ETM+) and Landsat 8 Operational Land Image (OLI) images of 1986, 2000 and 2018 sequentially were adopted. The maximum likelihood algorithm classifiers were used in generating the land use land cover. Three land use land cover were generated and they are; vegetation cover, built up area and waterbodies. The normalized difference vegetation index (NDVI) was calculated using near infrared (Band 5) and Red (Band4) bands. Land surface temperature data were acquired through the landsat infrared thermal bands for the three years and the relationship between NDVI and land surface temperature was analysed. The result of this study showed that there is a great decrease in the natural environment and an increase in developed environment from 1986 to 2018. The GIS analysis showed that built up area has 629.73% increase within the study period while the maximum surface temperature has risen with 7oC from 1986 to 2018. If the increase in built up area still prevails in the study area as mentioned above surface temperature will be on the high side and this may bring about urban heat island. Hence, growing of trees and vegetation in and around the study area should be encouraged so as to reduce the rise in surface temperature of the land cover in the greater Port Harcourt.

Keywords: Urban growth, landcover, thermal characteristics, surface temperature, land use

INTRODUCTION

Urban population has experienced a substantial increase in the last 30 years and the latest estimate indicates that in 2011 it amounted to more than half of the total world population [1]. The global percentage is projected to exceed 65 % of the total population by 2050. The growth of urban population has increasingly drawn the scientific community's attention to urban climate and the effects of urbanization at different scales [2], [3], [4], [5], [6], [7], [8], [9], [10], [11], [12], [13], [14] and [15]. Urban growth is not merely a modern phenomenon, but rapid and historic transformation replaced by predominantly urban culture [6]. This unprecedented movement of people is forecasted to continue and intensify in the next few decades. The process of urbanization is increasing in both the developed and developing

countries. However, rapid urbanization in particular the growth of large cities and the associated problems of unemployment, poverty, inadequate health, poor sanitation, urban slums and environmental degradation pose a formidable challenge in many developing countries especially in Greater Port Harcourt region.

The rapid growth in human population and economic output per capita has been unprecedented features of this industrial era [16] and [17]. This trend poses economic consequences on the global environment over the past century [18]. Urban expansion enhances heat-stress increases due to climate change at night, but partly compensates its effects during the day [19], [20], [21]. These differences are due to a stronger contribution from vapor pressure deficit during the day and from temperature increases during the night

induced by urban surfaces [22], [23], [24], [25], [26] and [22].

The so called Urban Heat Island (UHI) is primarily caused by the heat-storing structures that increase the heat capacity of the cities. Some studies have also identified the anthropogenic heat sources as an important contributor to this warming [27], [28] especially in regions of intense energy consumption and low net radiation. The imperviousness of urban surfaces was also found to enhance the UHI through inhibition of evaporative cooling [29], [30], [31], [32] and [33].

The replacement of the natural landscape by buildings and paved surfaces alters the aerodynamic properties (aerodynamic roughness) and radiative surface (albedo and effective emissivity), thermal properties of the substrate (capacity, conductivity and thermal admittance), and the hydraulic properties of the soil surface (surface permeability, hydraulic capacity and hydraulic conductivity) [34], [25], [35] and [36]. In large urban centers, the reduction of green areas and modifications occurred on the soil surface causes an increase of the surface and air temperature in contact with that surface. According to [37], although there is a reduction in radiative balance, since these changes in land occupation increases albedo and Surface Temperature (Ts), a large amount of radiation that was used in the evaporation of water from soil and vegetation, is now employed in the heating of soil and air. This effect is most evident in water mirrors, which have low albedo and although they have high radiative balance, the greater number is applied to the evaporation of water, resulting in very low Ts.

The surface temperature (Ts) has significant scientific importance in climatology and urbanization, as in the modeling of the energy balance [38] and biophysical and bioclimatic parameters of the surface. Thus, its estimation is of great utility in monitoring study of urban climate, and may contribute to the identification of changes in climatic elements in the urban environment [39].

Through thermal images obtained through remote sensing is possible to detect thermal characteristics of urban surface [40]. One of the main applications of remote sensing in the study of urban climates is to analyze the relation between the spatial structure of the urban thermal patterns and urban surface characteristics, which can assist the planning of the use and occupation of land [41].

The role of the replacement of vegetation cover resulting from the urbanization process has been well documented in the literature [42], [43], [44], [45], [46] and [47]. These studies suggest that the countryside or the suburbs of the metropolis, have greater radiative balance, but portion of it is used in the evaporation of water retained in the soil and vegetation. Thus, is evidenced in anthropic urban areas a substantial increase in surface and air temperatures [37], [48], [49] and [50]. A cursory examination of the literature reveals that no known study has examined the issue of temperature dynamics arising from urban growth in the Greater Port Harcourt Region especially with the invading of the region by property developers that have led to the emergence of such estates like De Dukes Court, Treasure Ville Layout, Quiet Heaven Layout Phase 1 and 2 among others. This is the gap this study intends to cover in the literature.

METHODOLOGY AND STUDY AREA

The data used for this study were obtained from secondary sources. The secondary sources included the downloading of Landsat satellite imageries for the landuse/land cover, surface temperature and Normalised Difference Vegetation Index (NDVI) which are the major parameters required in this study. The satellite imageries were downloaded from the website of United States Geological Survey (USGS) website and they included Landsat 5 Thematic Mapper (TM) for 1986, Landsat 7 Enhanced TM for 2000 and Landsat 8 Operational Land Imager (OLI)/Thermal Infrared Sensor (TIRS) for 2018. Also, the administrative map of Greater Port Harcourt was obtained from the Rivers State Ministry of Land and Housing, Port Harcourt (see fig. 1). The administrative map of Greater Port Harcourt was used to delineate the boundary of the study location and to carve out the study portion from the entire scene of the imagery. Greater Port Harcourt Region is in the South-South zone and Niger Delta area of Nigeria located within Latitudes 4°05'30''N and 5°14'25''N and Longitudes 5°40'30''E and 7°11'01''E of the Greenwich Meridian (GM). Greater Port Harcourt (also called Greater Port Harcourt City) is a metropolitan area currently under construction in Rivers State, Nigeria. It comprises the local government areas of Port Harcourt, Oyigbo, Okrika, Ogu-Bolo, Obio-Akpor, Ikwerre, Etche and Eleme. It covers an area of approximately 1,900 km² (734 mi²) and as of 2009 had a population of 2 million people. Major plans have been made to build the planned metro area through implementing and

The Algorithms of Urban Sprawl Dynamics on Surface Temperature Characteristics of Greater Port Harcourt Region, Using Remote Sensing- GIS Approach

enforcing infrastructural development and service delivery policies geared to improving the standard of living and well-being of the people. The key anchors of the new metro area include Port Harcourt International Airport, Port Harcourt City, and Port of One (Rivers State Government, 2009). Greater Port Harcourt City Development Authority (GPHCDA) is a regulatory body established by law with mandate to facilitate the implementation of the Greater Port Harcourt Master Plan and build the new Greater Port Harcourt City [51]. Climatologically, both the maritime and continental air masses control the rainfall and temperature pattern of the region. Also, as a city located within the Inter-Tropical Convergence Zone (ITCZ) in the African continent, it is affected with the warm humid maritime tropical air mass with its south-western winds and the hot and dry continental air mass from the north-easterly winds. The moist south-west wind in

the area generates heavy rainfall volumes ranging from 2000 mm to 2500 mm with the peak period from April to September and in some years, extends to October. From April, relative humidity increases, peaking in July to September and dropping steadily and continuously till March with the lowest trough in January [52]. The average daily sunshine was less than 3 hours as observed in July and about 4-5 hours in January and December respectively [53]. Soil unit (E) is made up of soils that are deep, porous and brown in colour. They have been formed on sandy parent materials, which are similar to the (F) and (G) soil associations. The difference between both groups arises from the fact that the (E) soil group is paler in colour because of intense leaching which is attendant on the heavy rainfall. Soil types here differ from sandy to sandy loam in surface characteristics. In the sub-surface, they become pervious brown sandy clay soil [54].

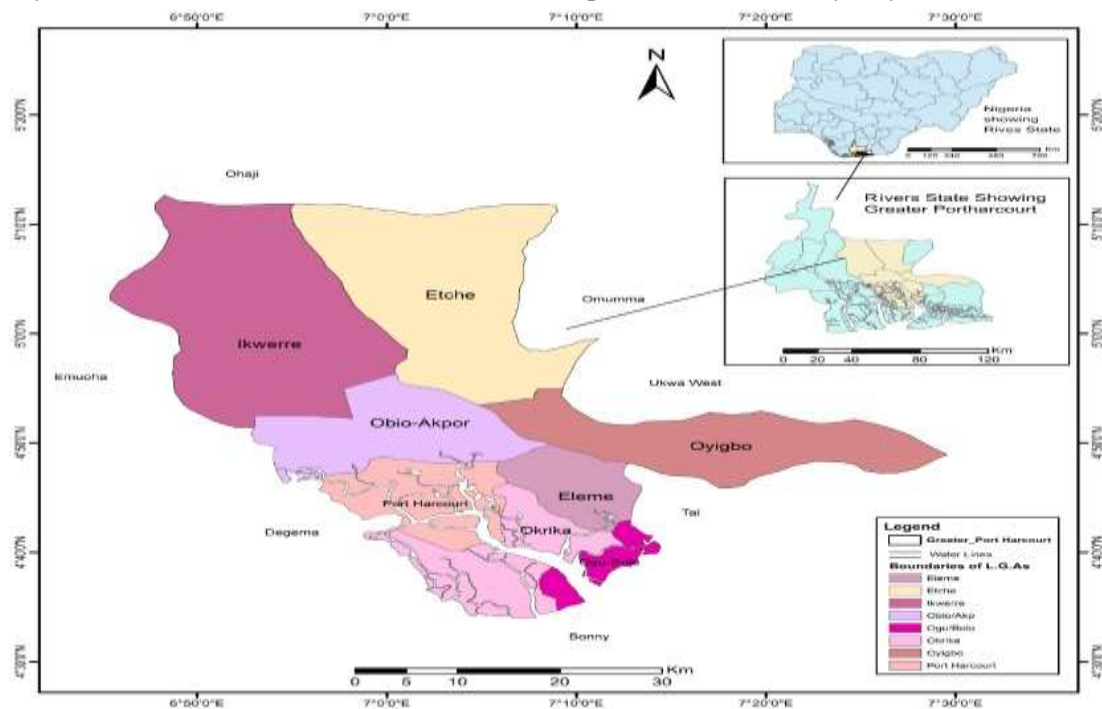


Fig1. Map of Greater Port Harcourt Region

Image Geo-Processing for Land Use Change and Percentage Change

The study made use of multi-spectral satellite images of Landsat 5 TM, Landsat 7 ETM and 8 OLI/TIRS of 1986, 2000 and 2018; all having some characteristics presented in Table 3.1. Landsat images were used because of their ability to have valuable and continuous records of the earth's surface for identifying and monitoring changes in man-made and physical environments [55]. The bands of the images were stacked together using COMPOSITE algorithm. Thereafter

supervised classification using maximum likelihood algorithm classifiers in [56] was used to classify similar spectral signatures into major classes which included vegetation cover, water bodies and built-up area (Table 1).

Maximum likelihood classifier was chosen because it is the most widely adopted parametric classification algorithm [57]. The area of each landuse class was computed in ArcGIS 10.5 which was used to compute the landuse change and percentage change in squared kilometers. The percentage change was computed using equation (1)

The Algorithms of Urban Sprawl Dynamics on Surface Temperature Characteristics of Greater Port Harcourt Region, Using Remote Sensing- GIS Approach

$$\left(\frac{d}{t_1}\right) * 100 \quad (1)$$

Where,

d is the difference in the value of area covered by a land cover category at the initial time point and final time point

t₁ is the value of the area covered by a land cover category in the initial time point

y₁ and y₂ are base year and final year respectively.

The following equation was used to convert the digital number (DN) of TIR bands of Landsat data into spectral radiance [30].

$$L\lambda = ((LMAX\lambda - LMIN\lambda)/(QCALMAX - QCALMIN)) * (QCAL - QCALMIN) + LMIN\lambda \quad (2)$$

Where:

Lλ = Spectral Radiance at the sensor's aperture in watts/(meter squared * ster * μm)

QCAL = the quantized calibrated pixel value in DN

LMINλ = the spectral radiance that is scaled to QCALMIN in watts/(meter squared * ster * μm)

LMAXλ = the spectral radiance that is scaled to QCALMAX in watts/(meter squared * ster * μm)
 QCALMINλ = the minimum quantized calibrated pixel value (corresponding to LMINλ)

QCALMAXλ = the maximum quantized calibrated pixel value (corresponding to LMAXλ).

See Table 2 for the values of LMAXλ, LMINλ, QCALMAXλ and QCALMINλ

To convert the spectral radiance values to brightness temperature, the equation below was used [30].

$$Tk = K2 \div \ln(K1 \div L\lambda + 1) \quad (3)$$

Where Tk is effective at-satellite temperature in Kelvin, Lk is spectral radiance in W/(m² sterμm); and K₂ and K₁ are pre-launch calibration constants. See Table 3.3 for values of K₁ and K₂.

Estimation of Surface Temperature of Land Use Land Cover Types

The analysis below showed the estimates of the surface temperature using the algorithms for detecting land use and cover change for different satellites.

Table1. Parameters for the Calculation of surface temperature

Satellite	Year	Band	LMAXλ	LMINλ	QCALMAXλ	QCALMINλ	K1	K2
Landsat5	1986	6	15.303	1.238	255	1	607.76	1260.6
Landsat7	2000	6L	17.04	0	255	1	666.09	1282.7
Landsat8	2018	10	22.0018	0.1003	65535	1	774.89	1321.1

To estimate the surface temperature (ST) of land use/cover types, 100 sample points were selected randomly from each land use land cover types in the study area. Geographic link and enquire cursor tools of ERDAS image 9.2 were used to

investigate the ST value of each sample point randomly selected. The average ST value for each land use land cover was calculated by taking the arithmetic mean of the values for each land use land cover.

Table2. Characteristics of Landsat Images

Year	Date Acquired	Sensor	Cloud Cover (%)	Path	Row	Resolution
1986	19/12/1986	Landsat 5TM	0	188	057	30m x 30m
2000	17/12/2000	Landsat 7 ETM	0	188	057	30m x 30m
2018	27/12/2018	Landsat 8 OLI/TIRS	0	188	057	30m x 30m

Source: U.S. Geological Survey, 2020

Table3. Landuse/Landcover Classification Scheme

S/N	Landuse Types	Description
1	Vegetation cover	Thick forest, Derived forest, mixed forest lands, palms, shrubs, herbs, agricultural area, crop fields, fallow lands and vegetable lands
2	Built Up Area	Residential, commercial and services, industrial, transportation, roads
3	Waterbodies	Rivers, permanent open water, lakes, ponds, reservoirs, etc

Sources: Adapted from [30]

Spatio-Temporal Land Surface Temperature

Land surface temperature data that were acquired from Landsat satellite infrared bands; Band 6

(10.40-12.50 um Thermal) of Landsat 5 TM; Band 6 (10.40-12.50 um Thermal) of Landsat 7 ETM+ and Band 10 (10.60-11.19 Thermal 1) of Landsat 8

The Algorithms of Urban Sprawl Dynamics on Surface Temperature Characteristics of Greater Port Harcourt Region, Using Remote Sensing- GIS Approach

OLI/TIRS; were used to investigate the land surface temperature and were guided by the procedure highlighted by [53] below:

- Top of Atmosphere (TOA) Radiance which involves using the radiance rescaling factor, to convert Thermal Infra-Red Digital Numbers to TOA spectral radiance.
- Top of Atmosphere (TOA) Brightness Temperature in which spectral radiance data shall be converted to top of atmosphere brightness temperature using the thermal constant values in metadata file.
- Normalized Differential Vegetation Index (NDVI) was calculated using Near Infra-red (Band 5) and Red (Band 4) bands.
- Land Surface Emissivity (LSE) which is the average emissivity of an element of the surface of the Earth calculated from NDVI values.

$$PV = [(NDVI - NDVI \min) / (NDVI \max + NDVI \min)]^2 \quad (4)$$

Where:

PV = Proportion of Vegetation

NDVI = DN values from NDVI Image

NDVI min = Minimum DN values from NDVI Image

NDVI max = Maximum DN values from NDVI Image

$$E = 0.004 * PV + 0.986 \quad (5)$$

Where:

E = Land Surface Emissivity

PV = Proportion of Vegetation

- Land Surface Temperature (LST) which is the radiative temperature that shall be calculated using Top of Atmosphere (TOA) brightness temperature, Wavelength of emitted radiance, and Land Surface Emissivity.

$$LST = (BT / 1) + W * (BT / 14388) * \ln(E) \quad (6)$$

Where:

BT = Top of atmosphere brightness temperature (°C)

W = Wavelength of emitted radiance

E = Land Surface Emissivity

RESULTS AND DISCUSSION OF FINDINGS

Landuse Change, Percentage Change and Urban Sprawl

Maps for the land use land cover for the three years' study period were generated and presented on maps. Fig. 2, 3 and 4 present the land use/ land cover for 1986, 2000 and 2018 while fig. 5, 6 and 7 were for 1986, 2000 and 2018 urban sprawl.

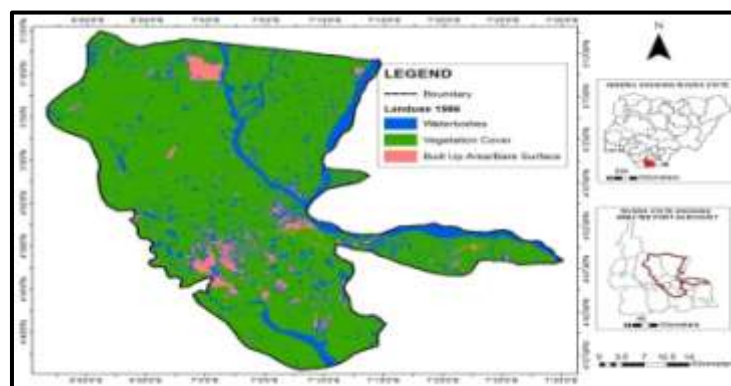


Fig2. Landuse/ Land cover of 1986

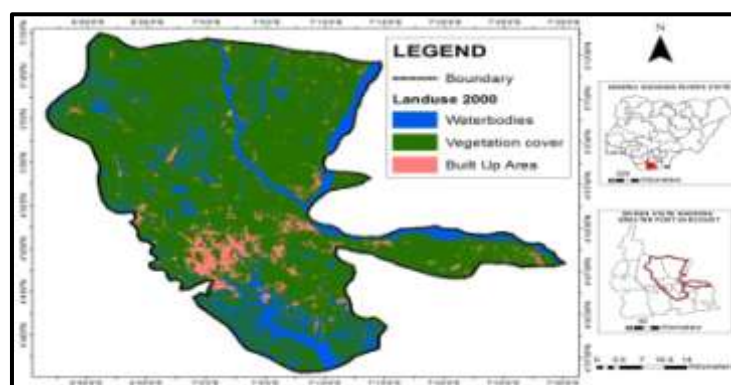


Fig3. Landuse/ Land cover of 2000

The Algorithms of Urban Sprawl Dynamics on Surface Temperature Characteristics of Greater Port Harcourt Region, Using Remote Sensing- GIS Approach

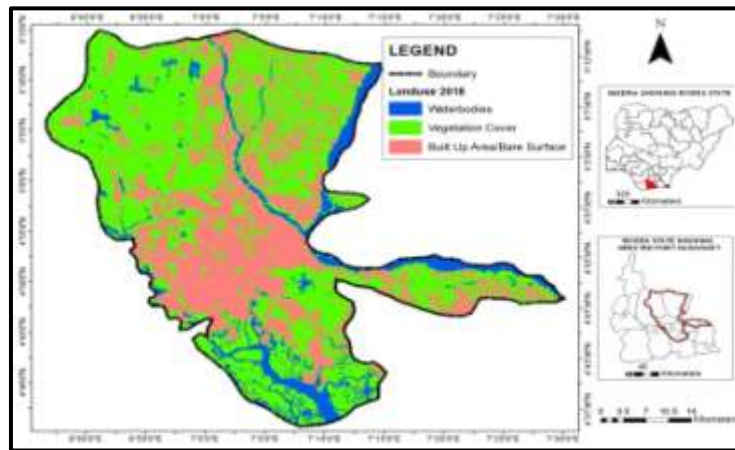


Fig4. Landuse/ Land cover of 2018

Table4. Landuse/Land covers Extent (1986-2018)

Landuse	1986 (sq km)	Percentage (%)	2000 (sq km)	Percentage (%)	2018 (sq km)	Percentage (%)
Waterbodies	416.36	16.48	413.29	16.36	259.74	10.28
Vegetation Cover	1992.44	78.88	1950.83	77.21	1407.12	55.69
Built Up Area	117.82	4.66	162.51	6.43	859.77	34.03
Total	2526.63	100	2526.63	100	2526.63	100

In the above table (4), the classification of landuse/land cover for 1986 from Landsat TM image (fig. 2) shows that most of the study area was under vegetation, which amounted to 1992.44 square kilometers (sqkms) which is 78.88% of the entire area. This is followed by water bodies; accounting for 416.36 sqkms (16.48%), while built up area occupies 117.82 sqkms (4.66%). The Landsat 7 ETM image for year 2000 landuse/land cover classification depicts that vegetation still has the highest percentage of the study area but

decreases to 77.21% (1950.83 sqkms), followed by water bodies and built up area with 16.39% (413.29 sq km) and 6.43% (162.51 sqkms) respectively. There was a slight decrease in the water bodies and increase in built up area. The result produced from 2018 Landsat 8 OLI/TIRS indicates that the dominant class is vegetation although it has inconsiderably decreased to 1407.12 sqkms (55.69%). Built up are increased to 859.77 sq.kms. (34.03%) while waterbodies reduced to 259.74 sqkms (10.28%).

Table5. Rate of Change and Percentage Change

Landuse	1986-2000	Percentage (%)	2000-2018 (sq km)	Percentage (%)	1986-2018	Percentage (%)
Waterbodies	-3.07	-0.73734	-153.55	-37.1531	-156.62	-37.6165
Vegetation Cover	-41.61	-2.08839	-543.71	-27.8707	-585.32	-29.377
Built Up Area	44.69	37.93074	697.26	429.0567	741.95	629.7318

Table 5. depicts the rate of changes in landuse/land cover change between the periods of 1986 to 2000, 2000 to 2018 and 1986 to 2018. The table 5 reveals that from 1986 to 2000, water bodies and vegetation cover had a decrease of 3.07 sqkms and 41.61 sqkms respectively while built up area recorded an increase with 44.69 sqkms. This could be induced by the numerous multinational oil and servicing company that exists in the city which allow a great influx of people in to the city. Therefore, private interests have greatly overcome the urban planning policies. Comparably, in the second phase of 2000 to 2018, built up areas also increased with 697.26 sqkms (429.0567%). Meanwhile, water bodies decreased with 153.35 sqkms (37.1531%) while vegetation cover also had

a decrease of 543.71 sqkms (27.8707%). In general, between 1986 to 2018 water bodies and vegetation cover decreased by 156.62 sqkms (37.6165%) and 585.32 sqkms (29.377%) respectively while the built-up area drastically increased by 741.95 sqkms (629.7318%) with the greatest increase occurring between 2000 to 2018 (429.0567%) when compared with the period of 1986 to 2000 (37.93074%).

Urban Sprawl Dynamics in the Greater Port Harcourt Region

This section presents the urban sprawl dynamics throughout the study period and the rate of changes within this period. The urban sprawl (1986-2018) and the rate of changes shown in

The Algorithms of Urban Sprawl Dynamics on Surface Temperature Characteristics of Greater Port Harcourt Region, Using Remote Sensing- GIS Approach

tables 5 and 6 refers to the data realized from fig. 5, 6 and 7. Fig 4.4 displays the Urban sprawl in

1986 while fig. 4.5 and 4.6 portray the urban sprawl in 2000 and 2018 respectively

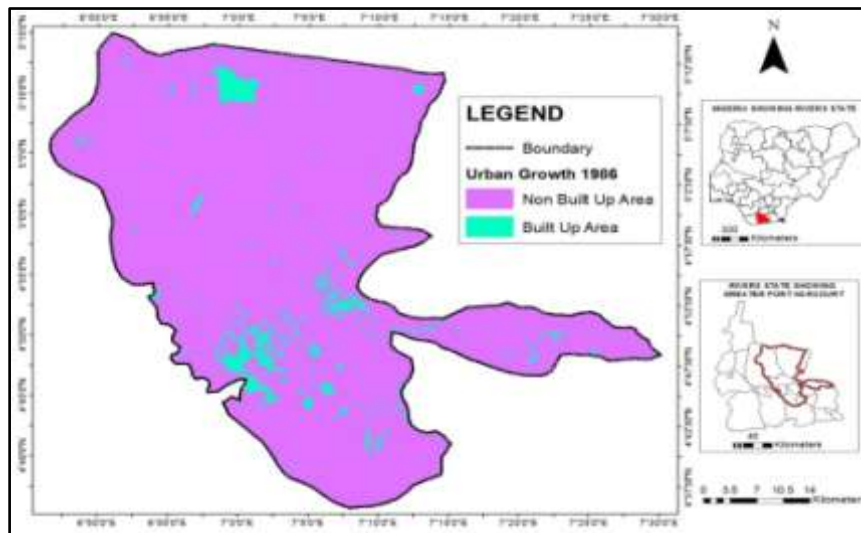


Fig5. Urban Sprawl in 1986.

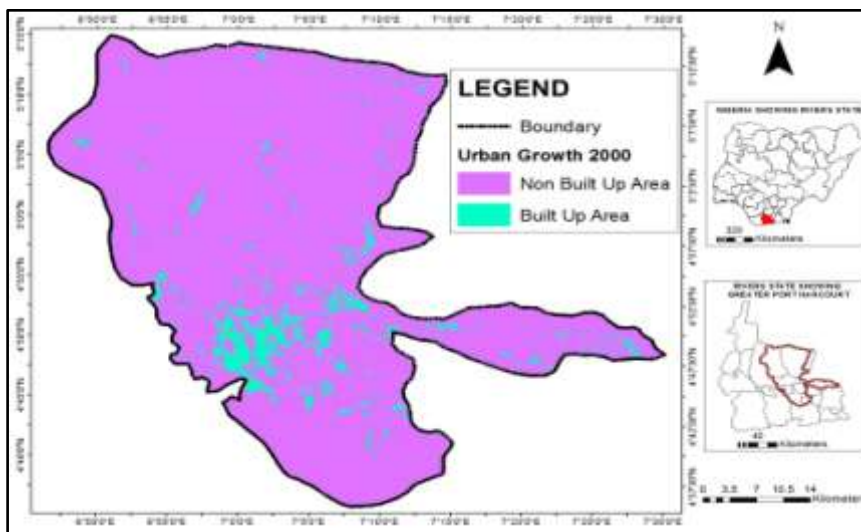


Fig6. Urban Sprawl in 2000

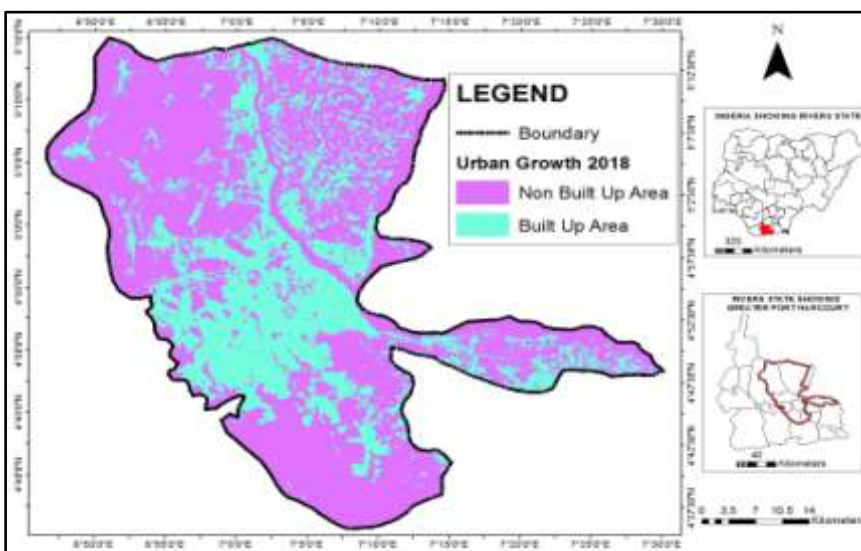


Fig7. Urban Sprawl in 2018

The Algorithms of Urban Sprawl Dynamics on Surface Temperature Characteristics of Greater Port Harcourt Region, Using Remote Sensing- GIS Approach

Table6. Urban Sprawl (1986-2018)

Landuse	1986	Percentage (%)	2000	Percentage (%)	2018	Percentage (%)
Non-Built Up Area	2408.81	95.34	2364.12	93.57	1666.74	65.97
Built Up Area	117.82	4.66	162.51	6.43	859.77	34.03
Total	2526.63	100	2526.63	100	2526.63	100

It could be seen in table 6 that in 1986 greater Port Harcourt city was mostly non-built up area which occupied 95.34% (2408.81 sqkms) of the entire area while built area has just 4.66% (117.82 sqkms). By the year 2000 non-built up

area decreased to 2364.12 sq km (93.57%) while built area increased to 162.51sq kms (6.43%). Also, non-built up area decreased to 1666.74 sqkms (6.5%) by the year 2018 while built area increased to 65.97 sq km (34.03%).

Table7. Rate of Change and Percentage Change of Urban Sprawl from 1986 to 2018

Landuse	1986-2000	Percentage (%)	2000-2018 (sq km)	Percentage (%)	1986-2018	Percentage (%)
Non-Built Up Area	-44.69	-1.85	1571.40	66.47	-742.07	-30.81
Built Up Area	44.69	37.93	855.11	526.19	741.95	629.73

According to table 7, non-built up area decreased with 44.69 sqkms (-1.85%) while built up area increased with also 44.69 sqkms (37.93%) from 1986 to 2000. From 2000 to 2018 built up recorded an increase with 855.11 (526.19%) and non-built area drastically reduced with 1571.4 sqkms (66.47%). Conclusively, from 1986 to 2018 non-built up area lost 742.47 sqkms (30.81%) while built up environment gained 741.95 sqkms (629.73%). This shows an upwelling urban sprawl and change in the morphology of the city size. The increase in i.e. settlement as well as infrastructural development like industrial plants, health, education and other socio economic reason resulted to these changes. Non-built up environment recorded its highest decrease from 2000 to 2018 with 66.47% while built up environment witnessed it highest increase from 2000 to 2018

with 526.19%. This increase in built up area within the study period shows that there is a great rise in the conversion of other landuses especially vegetation cover to built-up areas during the 32 years (1986 to 2018) as a result of urban growth within the city. Apart from the tables (4, 5, 6, and 7) presented above, the image classification result and visual comparison (fig. 2, 3, 4, 5, 6 and 7) show a great view into the immensity of the outlined classes of landscape and its changes observed.

The Normalized Differential Vegetation Index (NDVI) and Proportion of Vegetation

This section deals with the normalized difference vegetation index (NDVI) and the proportion of vegetation in the study area for the period of study

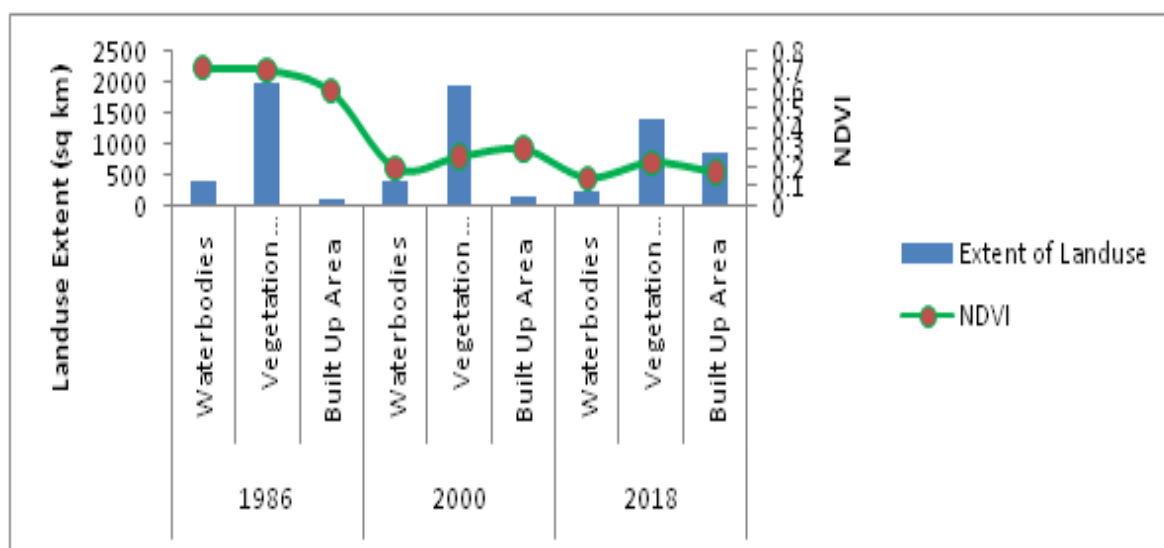


Fig8. NDVI and Extent of Landuse in the Major Landuse from 1986 to 2018

Table8. NDVI in the Major Landuse

Landuse	Min	Max	Mean	Standard Deviation
1986				
Water-bodies	-0.21	0.50	0.711	0.23
Vegetation Cover	-0.20	0.50	0.704	0.14
Built Up Area	-0.13	0.46	0.59	0.05
2000				
Water-bodies	-0.06	0.43	0.19	0.06
Vegetation Cover	-0.02	0.52	0.25	0.08
Built Up Area	-0.03	0.61	0.29	0.02
2018				
Water-bodies	-0.06	0.36	0.14	0.12
Vegetation Cover	-0.04	0.38	0.22	0.06
Built Up Area	-0.03	0.34	0.17	0.06

In table 8, water bodies have a min NDVI of -0.21 while vegetation cover and built up are have -0.21 and -0.13 respectively in 1986. The max NDVI recorded in 1986 was 0.50, 0.50 and 0.46 for water bodies, vegetation cover and built up area respectively. In 2000, water bodies exhibited a min, max and mean NDVI of -0.06, 0.43 and 0.19. Vegetation cover amounted to -0.02 and 0.52 for the min and max NDVI with a reduction in its NDVI mean and standard deviation (0.25 and 0.08). The table (4.5) also demonstrated that the min, max and mean NDVI for the built-up area increased to -0.03, 0.61 and

0.29 respectively. Water bodies maintained a min NDVI of -0.06 in 2018, a decrease in both max and mean (0.36 and 0.14) NDVI with a standard deviation of 0.12. Vegetation cover also decreases with -0.04, 0.38 and 0.22 for the min, max and mean NDVI. Built up area on the other hand also maintained a min NDVI of -0.03, a reduction in max NDVI and a decrease in mean NDVI (0.71) for 2018. This rapid decrease in NDVI is because of deforestation, conversion of green surfaces into built up areas (industrial, residential, commercial and services and transportation roads) promoted by urban sprawl.

Table9. NDVI in the Built-Up Area and Non-Built Up Area

Landuse	Min	Max	Mean	Standard Deviation
1986				
Non-Built Up Area	-0.21	0.50	0.295	0.01
Built Up Area	-0.13	0.46	0.202	0.11
2000				
Non-Built Up Area	-0.06	0.52	0.23	0.08
Built Up Area	-0.03	0.61	0.29	0.05
2018				
Non-Built Up Area	-0.06	0.38	0.21	0.08
Built Up Area	-0.03	0.34	0.17	0.06

As shown in table 9, non-built up area has a min, max and mean NDVI of -0.21, 0.50 and 0.295 respectively whereas built up area has -0.13, 0.46 and 0.202 for min, max and mean NDVI respectively for 1986. The year 2000 displays a slight increase in NDVI for both non-built up area (-0.06; min, 0.52; max and 0.23; mean). In 2018, non-built up area maintained the same min NDVI with that of year 2000 (-0.06) with a decrease in both max (0.38) and mean (0.21) NDVI. Built up area on the other hand has the same min NDVI for both 2000 and 2018 (-0.03) with a drastic reduction in both max (0.34) and mean (0.71) NDVI for 2018. The section below

examines Land surface temperature and its relationship to the incidence of Urban Sprawl in Greater Port Harcourt Region.

Land Surface Temperature (LST) Characteristics

In this segment, land surface temperature within the study period was presented and discussed. The data gotten from the Landsat images of figs. 9, 10 and 11, are presented on tables 10 and 11. Table 10 shows LST in the major landuses which are; water-bodies, vegetation cover and built up area. Conversely, table 10 exhibits the land surface temperature in the built-up area and non-built up area landuse.

The Algorithms of Urban Sprawl Dynamics on Surface Temperature Characteristics of Greater Port Harcourt Region, Using Remote Sensing- GIS Approach

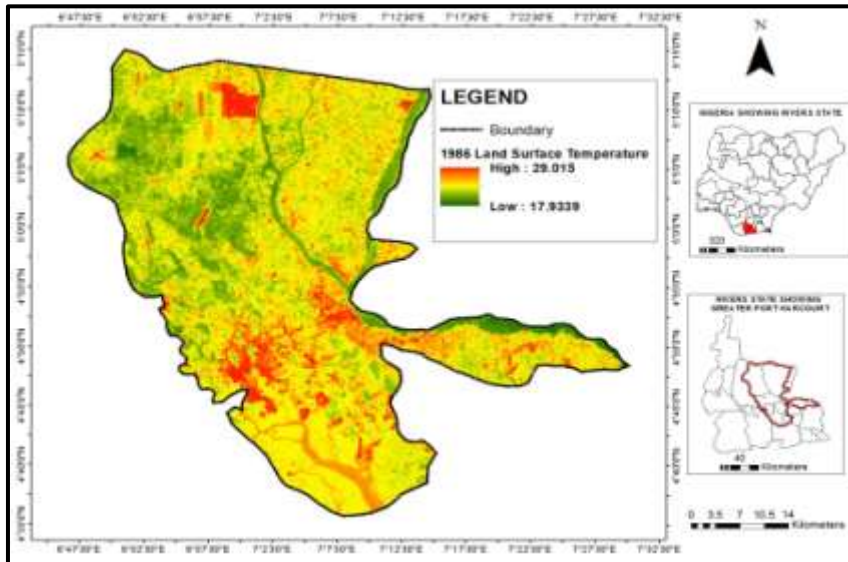


Fig9. Land Surface Temperature in 1986

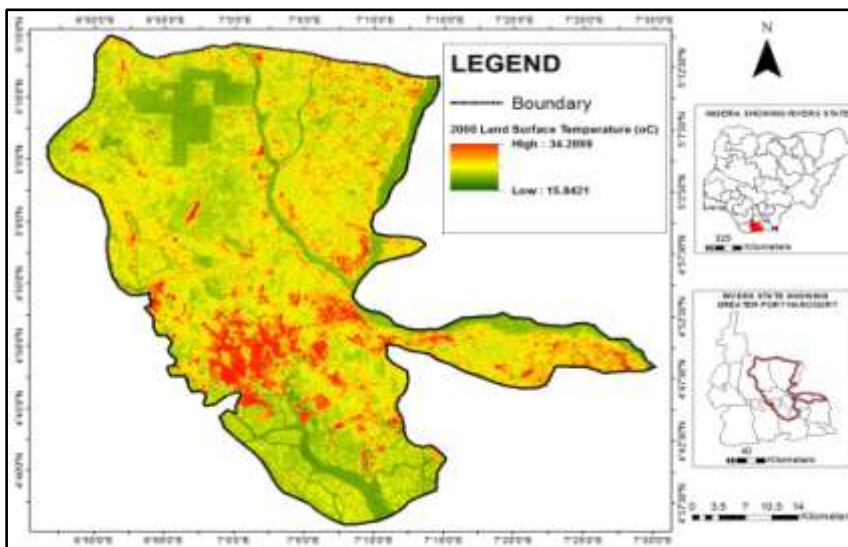


Fig10. Land Surface Temperature in 2000

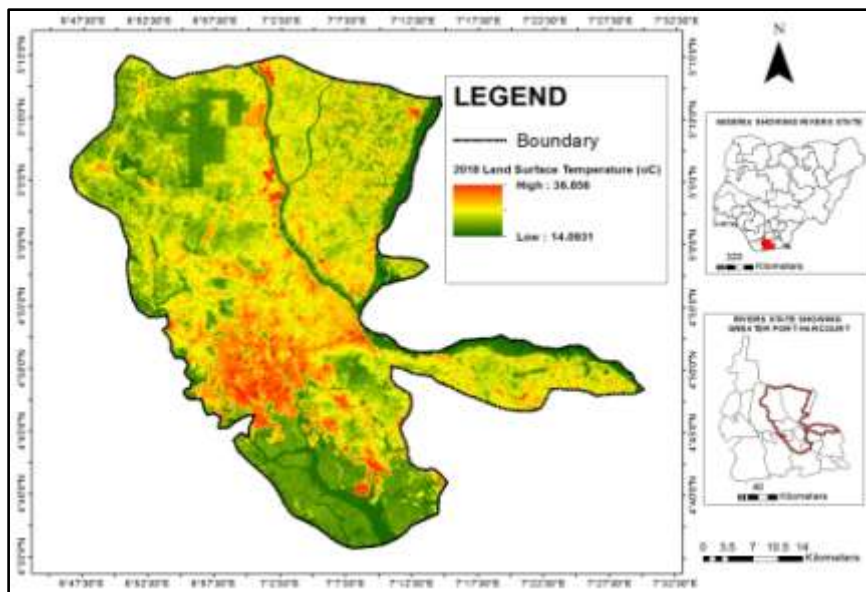


Fig11. Land Surface Temperature in 2018.

The Algorithms of Urban Sprawl Dynamics on Surface Temperature Characteristics of Greater Port Harcourt Region, Using Remote Sensing- GIS Approach

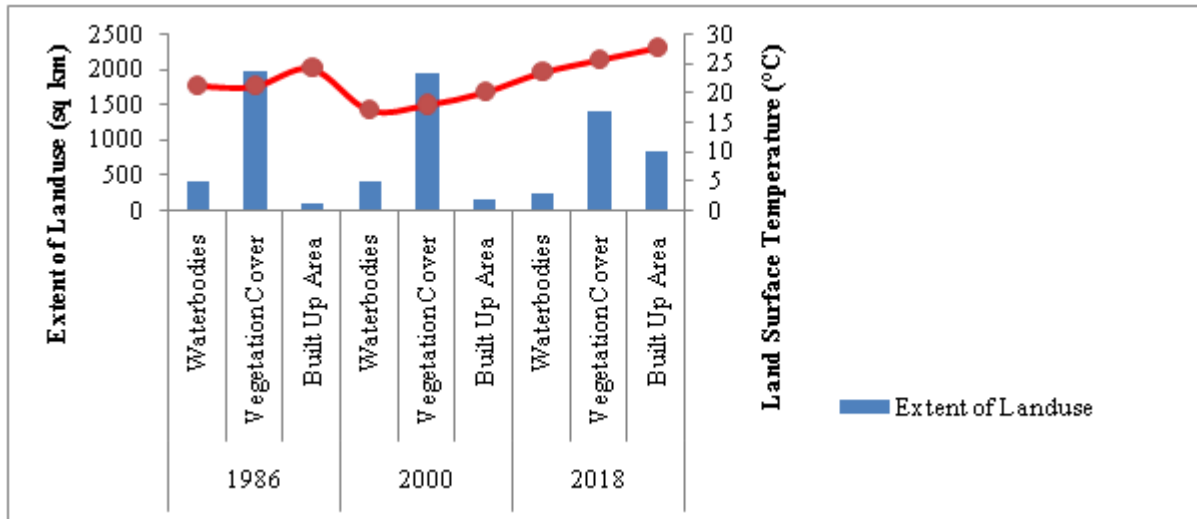


Fig12. Land Surface Temperature in the Major Landuse from 1986 to 2018

Table10. Land surface Temperature in the major Landuse

Landuse	Min	Max	Mean	Standard Deviation
1986				
Waterbodies	17.934	24.551	21.339	1.55
Vegetation Cover	18.836	23.689	21.204	0.71
Built Up Area	22.821	29.015	24.271	0.68
2000				
Waterbodies	15.84	18.22	17.21	0.21
Vegetation Cover	16.44	20.84	18.07	0.53
Built Up Area	18.22	34.20	20.21	0.57
2018				
Waterbodies	15.45	25.23	23.59	0.35
Vegetation Cover	22.82	28.13	25.75	0.73
Built Up Area	14.09	36.86	27.79	0.98

From table 10, it's obvious that waterbodies, vegetation and built up area recorded a min LST of 17.934°C, 18.836°C and 22.821°C respectively in 1986. In 2000, waterbodies have min LST of 15.84°C while vegetation cover and built up area have 16.44°C and 18.22°C exclusively. Equally, vegetation cover, waterbodies and built area exhibit a min LST of 22.82°C, 15.45°C and 14.09°C respectively in 2018. Table 9 likewise shows that among the various landuses, built up area had the highest max LST (29.015°C in 1986, 34.20°C in 2000 and 36.86°C in 2018). This is followed by vegetation cover (23.689°C in 1986, 20.84°C in 2000 and 28.13°C in 2018). In 1986, 2000 and 2018 the values of max LST exhibited by water-bodies are 24.551°C, 18.22°C and 25.23°C accordingly. Furthermore, water-bodies

record the lowest mean LST temp (21.339°C in 1986, 17.21°C in 2000 and 23.59°C in 2018) followed by vegetation cover (21.204°C in 1986, 18.07°C in 2000 and 27.79°C in 2018). Built up area, likewise exhibited the highest mean LST (21.339°C in 1986, 17.21°C in 2000 and 23.59°C in 2018).LST in the major landuse has a standard deviation of 1.55, 0.71 and 0.68 for water-bodies, vegetation cove and built up area for 1986. In 2000, the standard deviation was 0.21, 0.53 and 0.57 for water-bodies, vegetation cover and built up area. In 2018, water-bodies exhibited LST standard deviation of 0.35, while vegetation cover had 0.73 with built up area having 0.98. The findings of this work corroborates with studies of [30], [45], [51] and [57].

Table11. Land surface Temperature in the Built-Up Area and Non-Built Up Area Landuse.

Landuse	Min	Max	Mean	Standard Deviation
1986				
Non-Built Up Area	17.93	26.25	21.23	0.92
Built Up Area	21.51	29.02	24.26	0.70
2000				

The Algorithms of Urban Sprawl Dynamics on Surface Temperature Characteristics of Greater Port Harcourt Region, Using Remote Sensing- GIS Approach

Non-Built Up Area	15.84	21.99	17.92	0.59
Built Up Area	18.22	34.21	20.19	0.58
2018				
Non-Built Up Area	15.45	28.13	25.08	0.24
Built Up Area	14.09	36.86	27.78	0.98

From table 11 revealed that in 1986 non-built up are recorded a min and max LST of 17.93°C and 26.25°C respectively, with an average LST of 21.23°C and a standard deviation of 0.92. Built up area recorded a min LST of 21.51°C, max LST of 29.02°C, mean LST of 24.26°C and a standard deviation of 0.07.

In 2000, the min LST temp of built up area reduced to 18.22°C while having an increment in max LST (34.21°C) with an average LST of 20.19 and a standard deviation of 0.58. Also, in 2000 non-built up area had a reduction in temperature (15.84°C; min, 21.99°C; max, 17.92°C; mean and 0.59; standard deviation). Non-built area in 2018 recorded 15.45°C, 28.13°C, 25.08°C and 0.24 for min, max, mean and standard deviation serially. Built up area on the flip side portrayed 14.09°C for min LST, 36.86 for max LST, 27.8°C for mean LST and a standard deviation of 0.98.

Relationship between NDVI and Land Surface Temperature (LST)

The analysis in Fig. 13 and Table 12 display the interactions between the land surface temperature and vegetation vigor (NDVI). It is shown that as the period was increasing; the land surface temperature continued to be rising while the vegetation vigor was decreasing especially after 1986. This is represented quantitatively in the correlation analysis whereby the correlation coefficient (r) between land surface temperature and NDVI was -0.200. This showed that land surface temperature correlated negatively with the NDVI suggesting that as land surface was increasing, the NDVI was decreasing; although the correlation was not significant at p<0.05. The coefficient of determination (R²) was 0.04 which shows that NDVI can explain only 4% of the variation in the land surface temperature in the study area within the period of this study. This means that several other factors not considered in this work accounts for 96% of the variation in LST.

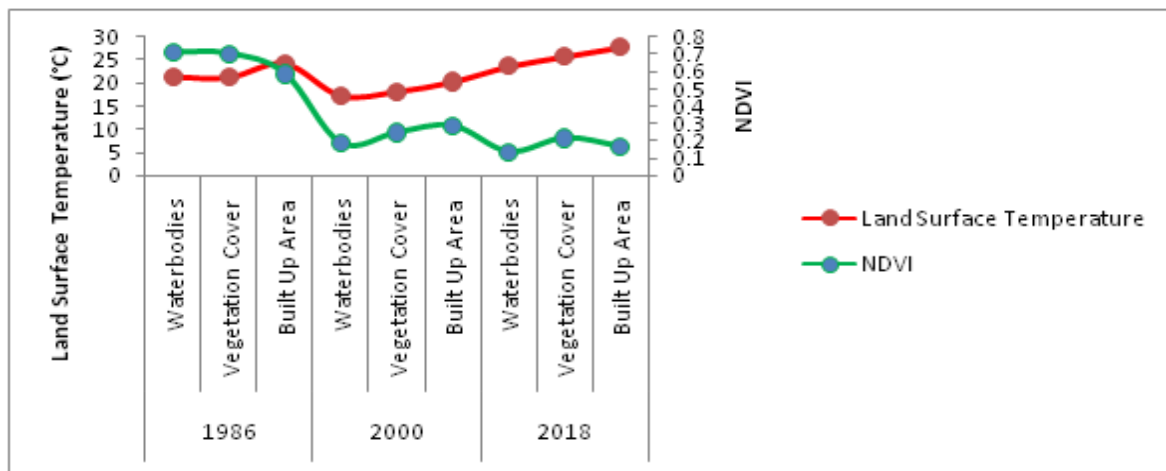


Fig13. NDVI and Land Surface Temperature across the Major Landuse from 1986 to 2018

Table12. Correlation between NDVI and Land Surface Temperature

			Land Surface Temperature (°C)	NDVI
Spearman's rho	Land Surface Temperature (°C)	Correlation Coefficient	1.000	-0.200
		Sig. (2-tailed)	.	0.606
		N	9	9

CONCLUSION

For the past 32 years, the Greater Port Harcourt has been undergoing intensified urban sprawl.

This study has proved the relevance of Landsat data in assessing the urban sprawl dynamics on surface temperature characteristics in the Greater Port Harcourt Region. Remote Sensing and GIS

algorithms were deployed to achieve the aim of the study. Finding showed that; natural surface generally experienced decline while developed surfaces increases from 1986 to 2018. From the GIS analysis, it showed that built up area has 629.73% increased from 1986 to 2018 while the max temperature had about 7°C increase within the study period. If the increase in built up area still prevails in the study area and vegetation continues to decline, surface temperature will be on the high side and this may result about urban heat island. However, further studies should focus on urban land use modeling and techniques integrating socio-economic data and GIS tools to forecast upcoming patterns of change. There should also be concentration on the effect of urban sprawl and growing built up areas on water pollution and stress etc.

REFERENCES

- [1] United Nations, Department of Economics and Social Affairs, Population Division (2019). World Population Prospects 2019: Highlights. ST/ESA/SER.A/423.
- [2] Kaufmann, R.K. K.C. Seto, A. Schneider, Z. Liu, L. Zhou, and W. Wang, (2007) "Climate response to rapid urban growth: evidence of a human-induced precipitation deficit," *Journal of Climate*, Vol. 20, no.10, pp.2299–2306, 2007.
- [3] Arnfield, A.J. (2003) "Two decades of urban climate research: a review of turbulence, exchanges of energy and water, and the urban heat Island," *International Journal of Climatology*, vol.23, no.1, pp.1–26.
- [4] Kalnay, E. and M. Cai. (2003) "Impact of urbanization and land-use change on climate". *Nature*, Vol.423, no.6939, Pp.528–531.
- [5] Childs, P. P, Raman, S (2005) Observations and numerical simulations of urban heat Island and Sea Breeze circulations over New York City. *Pure Appl Geophys* 162:1955–1980. doi:10.1007/s00024005- 2700-0
- [6] Gu, C. L. Hu, X. Zhang, X. Wang, and J. Guo, (2011) "Climate change and urbanization in the Yangtze River Delta," *Habitat International*, Vol.35, nN.4, Pp.544–552, 2011.
- [7] Grimmond C.S.B. (2007) Progress in measuring and observing the urban atmosphere. *Theor. Appl. Climatol.* 84:3–22. doi:10.1007/s00704-005-0140-5.
- [8] Kusaka H, Takata T, Takane Y (2010) Reproducibility of Regional climate in central Japan using the 4-km Resolution WRF Model. *Sola* 6:113–116. doi:10.2151/sola.2010-029.
- [9] Arguëso D, Hidalgo-Munõz JM, Gámiz-Fortis, S.R. (2011) Evaluation of WRF parameterizations for climate studies over Southern Spain using a multi-step regionalization. *J Clim* 24:5633–5651. doi:10.1175/JCLI-D-11-00073.1.
- [10] Wagner S, Berg P, Schärdler G, Kunstmann H (2012) High resolution regional climate model simulations for Germany: part II— projected climate changes. *Clim Dyn.* doi:10.1007/s00382012-1510-1.
- [11] Kusaka H, Hara M, Takane Y (2012a) Urban climate projection by the WRF model at 3-km horizontal grid increment: dynamical downscaling and predicting heat stress in the 2070's August for Tokyo, Osaka, and Nagoya Metropolises. *J Meteorol. Soc. Jpn.* 90B:47–63. doi:10.2151/jmsj.2012-B04.
- [12] Nwaerema P; T. E. Ologunorisa, M. O. Nwagbara, and Ojeh N. V. (2019a) Geo-Spatial Dynamics of Land Surface Temperature of Port Harcourt Metropolis and Environs: Implication for Heat Disaster Management. *Earth Sciences*. Vol. 8, No. 3, 2019, pp. 169-177. doi: 10.11648/j.earth.20190803.15.
- [13] Nwaerema, P; M. O. Nwagbara (2019) Assessment of Normalized Difference Vegetation Index (NDVI) of Port Harcourt Metropolis and Environs, from 1986 to 2018: Implication to Urban Greening and Management. *Annals of Geographical Studies*. Volume 2, Issue 2, 2019, PP 25-34
- [14] Nwaerema, P; Ojeh N. V, C. Amadou and Atuma, I. M. (2019) Spatial Assessment of Land Surface Temperature and Emissivity in the Tropical Littoral City of Port Harcourt, Nigeria. *International Journal of Environment and Climate Change* 9(2): 88-103, ISSN: 2581-8627.
- [15] Fashae, O.A., Adagbasa, E.G., Olusola, A.O. (2020) Land use/land cover change and land surface temperature of Ibadan and environs, Nigeria. *Environ Monit Assess* 192, 109. https://doi.org/10.1007/s10661-019-8054-3.
- [16] Stathopoulou, M. and Cartalis, C. (2006). Daytime urban heat islands from Landsat ETM+ and Corine land cover data: an application to major cities in Greece. *Solar Energy, Greece J*, 81, 358-368.
- [17] Hart, M. and Sailor, D. (2009). Quantifying the influence of land-use and surface characteristics on spatial variability in the urban heat island. *Theoretical and Applied Climatology* 95, 397-406. Available from: https://asu.pure.elsevier.com/.../quantifying-the-influence-of-land-use-and-surface-cha.
- [18] Ifatimehin, O. O; Ujoh, F. and Magaji, J.Y. (2009). An evaluation of the effect of Land use/cover change on the surface temperature of Lokoja town, Nigeria. *African Journal of Environmental Science and*, 86-90.
- [19] Deng, X, J. Huang, S. Rozelle, and E. Uchida, (2008) "Growth, population and industrialization,

- and urban land expansion of China,” *Journal of Urban Economics*, Vol.63, No.1, pp.96–115,2008.
- [20] Kusaka H, Kimura F (2004a) Coupling a single-layer urban canopy model with a simple atmospheric model: impact on urban heat island simulation for an idealized case. *J Meteorol SocJpn* 82:67–80
- [21] Wang, Q, D. Riemann, S. Vogt and R. Glaser (2014) “Impacts of land cover changes on climate trends in Jiangxi province China,” *International Journal of Biometeorology*, Vol.58, No.5. Pp.645– 660.
- [22] Pielke Sr. R.P, G. Marland, R.A. Bett. (2002) “The influence of land-use change and landscape dynamics on the climate system: Relevance to climate-change policy beyond the radiative effect of greenhouse gases,” *Philosophical Transactions of the Royal Society A: Mathematical, Physical and Engineering Sciences*, vol. 360, No.1797, pp.1705–1719.
- [23] Voogt, J. & Oke, T.R. (2003). Thermal Remote Sensing of Urban Areas. *Remote Sensing of Environment Journal*, 86: 370–384.
- [24] Li, M., J. Wu, and X. Deng,(2013) “Identifying drivers of land use change in China: a spatial multinomial logit model analysis,” *Land Economics*, vol.89, no.4, pp.632–654.
- [25] Pathirana, A, H, B. Deneke, W. Veerbeek, C. Zevenbergen, and A.T. Banda, (2014) “Impact of urban growth-driven land use change on microclimate and extreme precipitation—a sensitivity study,” *Atmospheric Research*, vol.138, pp.59–72.
- [26] Woldemichael, A.T, F. Hossain, and R. Pielke Sr.(2014) “Impacts of post-dam land use/land cover changes on modification of extreme precipitation in contrasting hydroclimate and terrain features,” *Journal of Hydrometeorology*, vol. 15, No. 2, pp. 777– 800,2014.
- [27] Kotani A, Sugita M. (2005) Seasonal variation of surface fluxes and scalar roughness of suburban land covers. *Journal of Agricultural and Forest Meteorology*. 2005; 135:1–21.
- [28] Weibo L, Johannes F, Leiqiu H, Ashley Z, Nathaniel B (2017). Seasonal and diurnal characteristics of land surface temperature and major explanatory factors in Harris County, Texas. *Sustainability*. 2017; 9: 2324. DOI: 10.3390/su9122324.
- [29] Lynn B. H, Carlson T. N, Rosenzweig C. (2009) A modification to the NOAA LSM to simulate heat mitigation strategies in theNew York City Metropolitan Area. *J Appl Met Clim* 48:199– 216. doi:10.1175/2008JAMC1774.1.
- [30] Zhang, N, Z. Q. Gao, X. M. Wang, and Y. Chen, (2010) “Modeling the impact of urbanization on the local and regional climate in Yangtze River Delta, China,” *Theoretical and Applied Climatology*, Vol.102, No.3-4, pp.331–342, 2010.
- [31] Forkes, J. ((2010)). *Urban Heat Island Mitigation in Canadian Communities*. Toronto, ON: Clean Air Partnership.
- [32] Giannaros, M and Melas.D. (2008). Climate change and extreme heat events. . *Am J Prev Med*, 429–435.
- [33] Singh, R.B, A. Grover, and J.Y. Zhan (2014) “Inter-seasonal variations of surface temperature in the urbanized environment of Delhi using Landsat thermal data,” *Energies*, vol.7, no.3, pp.1811–1828.
- [34] Ferreira, M.J.; Oliveira, A.P.; Soares, J.; Codato, G.; Bárbaro, E.W.; Escobedo, J.F. (2012) Radiation balance at the surface in the city of São Paulo, Brazil: diurnal and seasonal variations. *Theoreticaland Applied Climatology*, Wien, v.107, n.1-2, p.229-246, 2012.
- [35] Xiao R, Weng, Q; Ouyang, Z, Li W, Schienke, E.W; Zhang, Z. (2008). Land surface temperature variation and major factors in Beijing, China. *Photogramm. Eng. Remote Sens*;74:451
- [36] Heisler, G.Grimmond, S., Grant, R.H. &Souch, C. (1994). Investigation of the influence of Chicago's urban forests on and air temperature within residential neighborhoods. *Northeast Forest Experiment*, . *ground up Journal*, Vol. 186, pp. 19-40.
- [37] Stone, B.Hess, J.J. &Frumkin, H. (2010). Urban form and extreme heat events: Are sprawling cities more vulnerable to climate change than compact cities? . *Environmental Health Perspectives*, 118 (10), 1425-1428.
- [38] Ifatimehin, O.O. (2007). An Assessment of urban Heat Island of Lokoja Town and Surroundings using Landsat ETM Data. . *FUTY Journal of the Environment*, 100-108.
- [39] Codato, G.; Oliveira, A.P.; Soares, J.; Escobedo, J.F.; Gomes, E.N.; Pai, A.D. (2008) Global and diffuse solar irradiances in urban and rural areas in southeast of Brazil. *Theoretical and Applied Climatology*, Wien, v.93, n.1-2, p.57-73.
- [40] Chander, G.; Markham, B.L.; Helder, D.L. (2009) Summary of current radiometric calibration coefficients for Landsat MSS, TM, ETM+, and EO-1 ALI sensors. *Remote Sensing of Environment*, Oxford, v.113, p.893-903.
- [41] Chen, X.L.; Zhao, H.M.; Li, P.X.; Yin, Z.Y. (2006) Remote sensing image-based analysis of the relationship between urban heat island and land use/cover changes. *Remote Sensing of Environment*, Oxford, v.104, p.133-146.
- [42] Mohan, M. Kikegawa, Y., Gurjar, B.R., Bhati, S. and Koll, N.R. (2009). Assessment of Urban Heat Island Intensities over Delhi. *The seventh International Conference on Urban Climate*, (pp. 235-398). 29 June - 3 July 2009, Yokohama, Japan.

The Algorithms of Urban Sprawl Dynamics on Surface Temperature Characteristics of Greater Port Harcourt Region, Using Remote Sensing- GIS Approach

- [43] Weng, Q. (2001). A remote sensing-GIS evaluation of urban expansion and its impact on surface temperature in the Zhujiang Delta, China. *International Journal of Remote Sensing*, 22(10), 1999-2014.
- [44] Kato, S.; Yamaguchi, Y. (2005) Analysis of urban heat-island effect using ASTER and ETM+ data: separation of anthropogenic heat discharge and natural heat radiation from sensible heat flux. *Remote Sensing of Environment*, Oxford, v.99, p.44-54.
- [45] Christen, A.; Vogt, R. (2004) Energy and radiation balance of a Central European city. *International Journal of Climatology*, Chichester, v.24, p.1.395-1.421, 2004.
- [46] Li, Z.H., Deng, X. Z, Huang, J. K. and Zhang, R.R. (2013) "Critical studies on integrating land-use induced effects on climate regulation services into impact assessment for human wellbeing," *Advances in Meteorology*, vol. 2013, Article ID 831250, 14pages.
- [47] Balogun A.A, Balogun I.A, Adefisan A.E, Abatan A.A (2018). Observed characteristics of the urban heat island during the harmattan and monsoon in Akure, Nigeria. Eight Conferences on the Urban Environment. AMS 89th Annual Meeting, 11 – 15 January, Phoenix, AZ. Paper JP4.6; 2018.
- [48] Zhao J, Wang N. (2002) Remote sensing analysis of urbanization effect on climate in Lanzhou. *Arid Land Geography*; 25(1):90-95.
- [49] David, P., Zina, M., Nektrarios, C. and Michael, A. (2017). Online Global Land Surface Temperature Estimation from Landsat. *Remote Sens.* 9 (12), 1208. doi.org/10.3390/rs9121208.
- [50] IPCC. (2013). Climate change : the Physical Science Basis. Contribution of working group I to the fifth assessment report of the intergovernmental panel on climate change. . *Cambridge University Press, Cambridge, United Kingdom and New York, NY, USA.*, 10-57.
- [51] Government of Rivers State of Nigeria, (2009) Greater Port Harcourt information booklet. Retrieved on 20th February, 2017 from Website: www.greaterphc.comTel:084-465650.
- [52] Weli, V.E. (2014) Atmospheric concentration of Particulates and its implications for Respiratory Health Hazard Management in Port Harcourt Metropolis, Nigeria. *Journal of Civil and Environmental Research*. Vol. 6, No. 5 Pp 11-17. USA.
- [53] Weli, V.E. and Efe, S.I. (2015) Climate change and Epidemiology of Malaria in Port Harcourt Region, Nigeria. *American Journal of Climate Change*, Vol. 4, No 1, pp 40-47. USA.
- [54] Weli, V.E., Adegoke, J. O. and Ndidi, O.C. (2016) Hydrological Modeling of Aquifers and Their Ground Water Potentials: Implications for Water Resources Planning and Management in Parts of Obio/Akpor L.G.A, Rivers State, Nigeria. *Journal of Water Resource and Protection*, No.3, 372-381. <http://dx.doi.org/10.4236/jwarp.2016.83031>. **China**.
- [55] Weng, Q; Liu H, Liang B, Lu D (2008). The spatial variations of urban land surface temperatures: Pertinent factors, zoning effect, and seasonal variability. *IEEE J. Sel. Top. Appl. Earth Obs. Remote Sens.* 2008; 1:154–166. DOI: 10.1109/JSTARS.2008.917869.
- [56] Owen, T.W., Carlson, T.N. & Cullies, R.R. (1998). An Assessment of Satellite Remotely-Sensed Land Cover Parameters in Quantitatively Describing the Climate effect of Urbanization. *International Journal of Remote Sensing*, 19, 1663-1681.
- [57] Morris, C., Simmond, I. & Plummer, N. (2001). Quantification of the Influences of Wind and Cloud on the Nocturnal Urban Heat Island of a Large City. *Journal of Applied Meteorology*, 40 (2) 162-181.
- [58] Mirzaei, P. A. (2015). *Recent Challenges in Modeling of Urban Heat Island. Sustainable Cities and Society*, 19, 200-206. <http://doi.org/10.1016/j.scs.2015.04.001>.

Citation: Vincent Ezikornwor Weli, Alexander Chibuzor Okoli, et.al., "The Algorithms of Urban Sprawl Dynamics on Surface Temperature Characteristics of Greater Port Harcourt Region, Using Remote Sensing- GIS Approach", *Annals of Geographical Studies*, 3(2), 2020, pp. 19-33.

Copyright: © 2020 Vincent Ezikornwor Weli. This is an open-access article distributed under the terms of the Creative Commons Attribution License, which permits unrestricted use, distribution, and reproduction in any medium, provided the original author and source are credited.